ELSEVIER

Coordination Chemistry Reviews
176 (1998) 87–112

COORDINATION CHEMISTRY REVIEWS

Charge transfer complexes and electron transfer reaction of organosilicon and related compounds

Masahiro Kako*, Ysahiro Nakadaira

Department of Chemistry, The University of Electro-Communications, Chofu, Tokyo 182, Japan

Received 7 October 1997; accepted 23 October 1997

Contents

Abstract

Charge transfer absorptions of linear oligosilanes and silanorbornadienes, charge transfer induced oligomerization, polymerization and cycloaddition of tetrasilacyclooctadiyne and its germanium analogues are described. Photo-induced electron transfer reactions of various

* Corresponding author.

PII S0010-8545(98)00145-3

types of organosilicon compounds are discussed in detail, and include photo-induced chlorinative Si–Si bond cleavage, photo-induced nucleophilic Si–Si bond cleavage, fluorinative Si–Si bond cleavage via electron transfer, skeletal rearrangement via photo-induced electron transfer and the structure of a silyl radical cation.

Keywords: Organosilicon compound; Organogermanium compound; Charge transfer complex; Photo-induced electron transfer

1. Introduction

Since silicon is located just below carbon, and both elements are in the same family in the periodic chart, in addition to penta- and hexavalent compounds and silicates, a silicon atom is able to form the same type of tetravalent compounds as carbon. However, silicon is a third row element but carbon belongs to the second row, so the silicon atom is much more positive and hence, in terms of ionization energy (IE), a Si–Si σ bond is similar to a C–C π bond rather than a C–C σ bond. Thus, Si–Si bonds have been known to show analogous chemical reactivity with that of C–C π bonds, and are able to conjugate with each other (σ–σ conjugation) as well. A Si–C σ bond has higher IE than that of a Si–Si σ bond, but it is still low enough to be able to conjugate with a C–C π bond effectively [1]. In fact, HOMOs of β-silylated olefin and aromatic compounds are significantly destabilized due to σ–π conjugation between the orbitals of C–C π bonds and Si–C σ bonds [2,3], and these compounds are commonly used as electron donors. These characteristics of a Si–Si and a Si–C σ bond have made the electron transfer chemistry of organosilicon and related compounds attractive and productive [4–29].

In general, organosilicon compounds having somewhat activated Si–Si or Si–C bonds undergo efficient electronic interaction with a strong electron acceptor, such as tetracyanoethylene (TCNE) to produce the charge transfer (CT) complex. Even when the acceptor is not strong enough to cause effective electronic interaction with the donor in the ground state such as 9,10-dicyanoanthracene (DCA), upon irradiation with an appropriate light source, the acceptor is excited to the singlet state, and then its electron accepting ability is highly enhanced [30–33]. Now, electron transfer between the two components occurs exothermally. Here we have reviewed principally our recent work in this area with emphasis on the Si–Si and Si–C bond cleavage reaction coupled with the structure and reactivity of the key intermediate, a silyl radical cation. Owing to the space limitation for review, the photo-induced alkylation and silylation of electron deficient aromatics, pyrylium salt and α-diketone by Group 14 metal alkyls and oligosilanes are not included here [6,7,34–38].

Table 1
Frequencies (cm^{-1}), wavelengths (nm), and ionization energies (IE) for charge transfer absorptions (λ_{max}) in complexes of TCNE with permethylpolysilanes **1** in CH_2Cl_2 at room temperature[a]

n	λ_{max} / cm^{-1}	λ_{max} / nm	IE(PE)[b]
2	24000	417	8.69
3	21100	474	8.19
4	19600	510	7.98
5	18400	543	(7.79)[c]

[a] Ref. [40].
[b] Ionization energies (eV) determined by a photoelectron spectroscopic method (PE).
[c] Calculated from the relationship between IE(EI)[d] and IE(PE) for linear permethylpolysilanes: IE(PE) = 1.009IE(EP) + 0.613 (r = 0.999).
[d] Ionization energies determined by electron impact.

2. Charge transfer complex of organosilicon and related compounds with some powerful electron acceptors

2.1. Charge transfer complex formation

By analogy with well-known CT complexes of π- and n-donors such as aromatic hydrocarbons and amines, with π-acceptors such as TCNE [39,40], permethylpolysilanes **1** ($n > 2$) serve as good σ-electron donors and interact with TCNE to give well-defined CT bands in the absorption spectra as listed in Table 1 [41,42]. Irradiation of the CT band induced electron transfer and gave the ESR signals assigned to TCNE radical anion [42]. The absorption maxima of the CT spectra for the TCNE complexes shifted to longer wavelengths as the polysilanyl chain increased, and a good linear relationship between CT frequencies and ionization energies (IEs) of the respective polysilanes was demonstrated (see footnote c of Table 1).

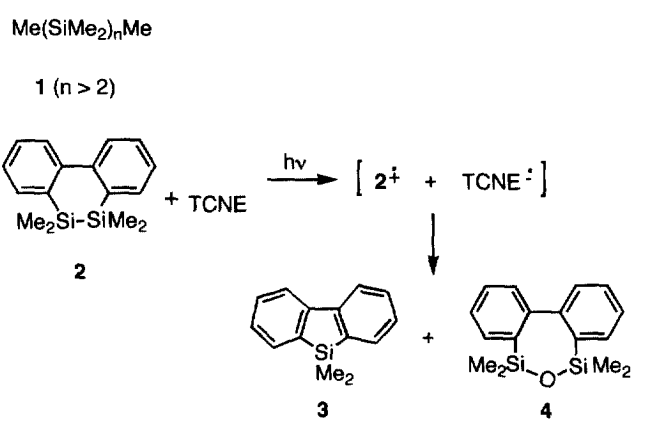

(1)

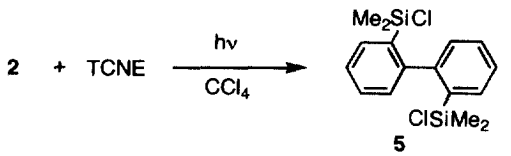

(2)

Generally, intramolecular and intermolecular CT interaction does not induce any chemical reaction but often produces a CT absorption band. Even irradiation of the CT band only causes efficient back and forth electron transfer within the donor–acceptor pair. In the case of dibenzodisilacyclohexadiene **2** having a Si–Si σ bond activated by ring strain, it showed two CT bands at 17900 and 23800 cm^{-1} (559 and 420 nm) in the presence of TCNE in CH_2Cl_2. The formation of a CT complex was evidenced by the fact that irradiation of the CT bands gave an ESR spectrum of TCNE radical anion at −90 °C. Interestingly, irradiation of **2** and an equimolar amount of TCNE in CH_2Cl_2 with a Na lamp (589 nm) at room temperature formed silafluorene **3** and disiloxane **4** [Eq. (1)] [43]. On the other hand, irradiation of **2** and TCNE (1:1) in the presence of a large excess of CCl_4 under similar conditions gave a chlorinated product 2,2′-bis(chlorodimethylsilyl)biphenyl (**5**) [Eq. (2)].

Silanorbornadienes **6a,b** have fairly low oxidation potentials (**6a**: E_{ox} = +1.45 V vs. SCE; **6b**: E_{ox} = +1.40 V vs. SCE) [44], upon mixing **6a** and TCNE in CH_2Cl_2, an intense coloration with an absorption maximum at 467 nm developed immediately. According to Mulliken's CT theory [45], the absorption bands of the CT complex shift to a longer wavelength as the magnitude of electron donating abilities of donors increases. Previously, **7a–c** and TCNE have been reported to

Table 2
UV absorption maxima of CT complexes of **6b** with some acceptors

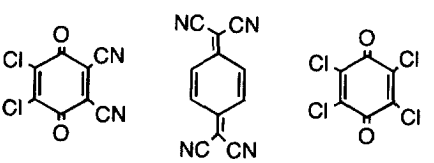

DDQ TCNQ CL

Acceptor	E_{red} (V) vs. SCE	λ_{CT} (nm)	$h\nu_{CT}$ (eV)
TCNE	+0.24	507	2.45
DDQ	+0.52	500	2.48
TCNQ	+0.18	445	2.79
CL	+0.04	420	2.95

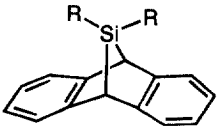

6a: R = 2,6-dimethylphenyl,
6b : R = mesityl

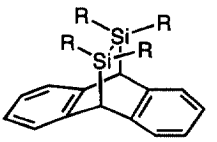

7a: R = Me, **7b**: R = ^{i}Pr,
7c: R = $CH_2{}^{t}Bu$

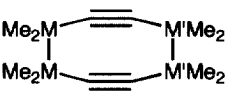

8a: M = M' = Si
8b: M = M' = Ge
8c: M = Si, M' = Ge

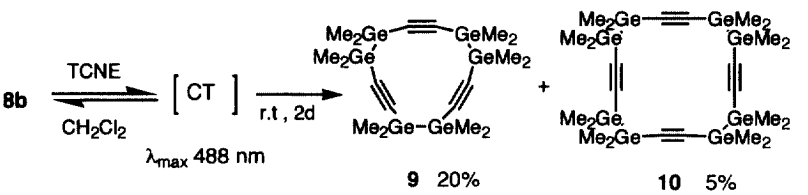

(3)

form CT complexes with absorption maxima at 630–650 nm, and the donor properties of **7a–c** are attributed to the effective overlapping of π-orbitals of the aromatic ring with the benzylic Si–C σ bonds [46–50]. Meanwhile, in comparison with **7**, such σ–π conjugation in **6** should be less effective because the dihedral angle between the π-orbital of the anthracene moiety and the benzylic Si–C σ bond is 43° (calculated by MOPAC PM3 method [51,52]), much larger than that of **7c** (17°) [50]. Similarly, **6b** and benzoquinone derivatives, chloranil (CL), tetracyanoquinodimethane (TCNQ), and dichlorodicyanobenzoquinone (DDQ) formed CT complexes having absorption maxima as summarized in Table 2. There seems to be a linear correlation between the charge transfer energies ($h\nu_{CT}$) and the reduction potentials (E_{red}) of acceptors for **6b**–quinone systems, as expected from Mulliken's CT theory [9,10,45].

2.2. Charge transfer induced oligomerization and polymerization

3,4,7,8-Tetrasilacycloocta-1,5-dyne **8a** shows characteristic electronic properties which are rationalized by through-bond conjugation among the two in-plane π-orbitals of ethynylenes and the two σ-orbitals of Si–Si bonds [53–55]. Recently, two corresponding germanium analogues, 3,4,7,8-tetragermacycloocta-1,5-diyne (**8b**) and 3,4-disila-7,8-digermacycloocta-1,5-diyne (**8c**) were prepared, respectively [56,57]. Similar to a Si–Si σ bond, the higher homologue Ge–Ge σ bond has been

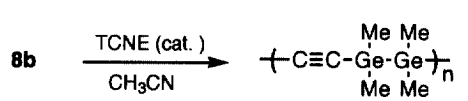

(4)

Table 3
Ionization energies (IE), intermolecular charge transfer absorptions (λ_{CT}) and UV absorption maxima (λ_{max}) of **8a**, **8b** and **8c**

Compound	IE (eV)[a]	λ_{CT} (nm)[b]	λ_{CT} (nm)[c]	λ_{max} (nm)(ε)[d]
8a	8.18, 9.48	462	516	251 (18500) 237 (sh 13900)
8b	8.00, 9.17	488	536	238 (17000) 228 (sh 11100)
8c	8.15, 9.36	467	519	244 (18200) 232 (sh 10900)

[a] Determined by PE spectroscopy [57].
[b] With TCNE in CH_2Cl_2.
[c] With DDQ in CH_2Cl_2.
[d] In cyclohexane.

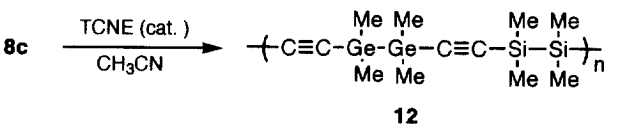

12 (5)

recognized to act as an efficient electron donor to form a CT complex with electron acceptors such as TCNE [58–61]. **8a,b** become coloured on mixing with TCNE (0.1–0.5 M) in CH_2Cl_2 to give characteristic intermolecular CT absorptions within

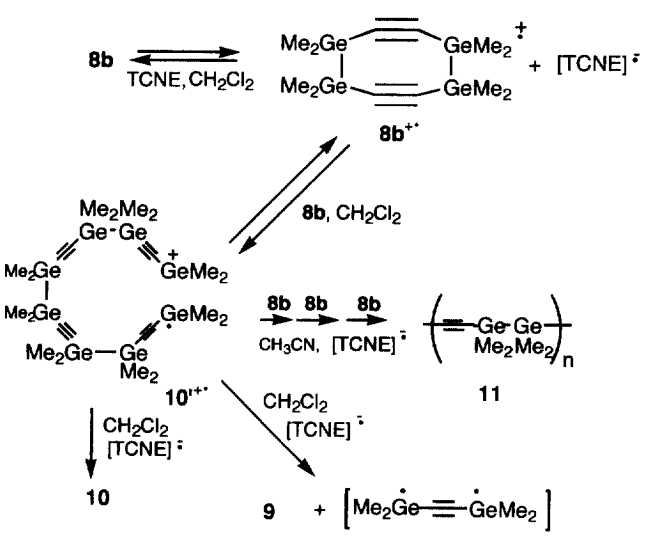

Scheme 1. Mechanism of oligomerization and polymerization of **8b**.

the visible region (Table 3). The intensities increase with increasing concentration of both ethynylene **8** and TCNE. The absorption maxima of the CT spectra are red shifted in the order of **8b**, **8c** and **8a** as the IE value of the donor decreases.

A Ge–Ge σ bond is more susceptible to electrophiles and, in fact, TCNE is inserted into the σ-Ge–Ge bond of polygermanes to give a 1:1 adduct under mild conditions [58–60]. Unlike the polygermane, **8b** turns out to be oligomerized in the presence of TCNE in CH_2Cl_2 at room temperature, possibly via a CT complex, to give higher homologues **9** and **10** in 20% and 5% yields, respectively [Eq. (3)] [57]. Interestingly, in the more polar solvent CH_3CN containing a catalytic amount of TCNE, **8b** and **8c** undergo ring-opening polymerization to give **11** and **12**, respectively, in almost quantitative yield [Eqs. (4),(5)]. However, under the reaction conditions **8a** shows only the CT maximum which is stable on prolonged standing even on irradiation of the CT band. These two polymers, **11** and **12**, show similar ^1H and ^{13}C NMR spectra to those of starting diynes **8b** and **8c**, respectively. In GPC analysis, both give one peak with $M_n = 5.0 \times 10^3$ ($M_w/M_n = 1.4$) and 4.4×10^3 ($M_w/M_n = 1.3$), respectively, based on the polystyrene standard. All the above data indicate that **11** and **12** should be a (digermanylene)(ethynylene) unit-containing polymer and an alternating (digermanylene)(ethynylene) and (disilanylene)(ethynylene) unit-containing polymer, respectively.

The mechanism of the oligomerization and polymerization of **8b** is not clear, but a plausible reaction pathway is depicted in Scheme 1. Thus, the first step probably involves electron transfer from **8b** to TCNE to form a radical ion pair, such as $\mathbf{8b}^{+\cdot}[TCNE]^{-\cdot}$. Then, since DDQ readily inserts into the Ge–Ge bonds of these cyclic ethynylenes as described below [see Eq. (6)], the dimerization of $\mathbf{8b}^{+\cdot}$ with **8b** should proceed with cleavage of the Ge–Ge bonds of both molecules involved, and this gives $\mathbf{10'}^{+\cdot}$ as a key intermediate. The chemical behaviour of $\mathbf{10'}^{+\cdot}$ is rationalized in terms of an open-chain structure in which the one-electron Ge–Ge bond dissociates to yield the cationic and radical ends, possibly with assistance of the solvent [61]. Back-electron transfer to $\mathbf{10'}^{+\cdot}$ from the TCNE radical anion forms the Ge–Ge bond again to yield **10**. On the other hand, the intramolecular cyclization affords **9** accompanied by elimination of a bis(germylethynylene) unit, possibly followed by back-electron transfer from the TCNE radical anion. In CH_3CN, $\mathbf{10'}^{+\cdot}$ reacts more readily with another molecule of **8b** in a similar way to give polymer **11**. The TCNE-catalyzed polymerization of **8c** in CH_3CN occurs more

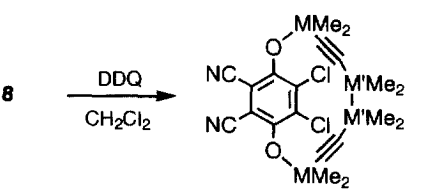

13: M = M' = Si, **14**: M = M' = Ge,
15: M = Si, M' = Ge, **16**: M = Ge, M' = Si (6)

slowly to give **12**, but it is conceivable that it proceeds by a similar mechanism to that above.

2.3. Charge transfer induced cycloaddition

On mixing with another acceptor DDQ in CH_2Cl_2, ethynylenes **8a–c** also show characteristic intermolecular CT absorption maxima even at longer wavelengths, namely 536, 519 and 516 nm, respectively (Table 3). However, in contrast to the case with TCNE above, a CH_2Cl_2 solution of **8a** and DDQ leads to the formation of [2 + 6] cycloadduct **13** on standing at ambient temperature [Eq. (6)]. Under similar conditions, **8b** and **8c** with DDQ yield the corresponding bridged adducts **14–16**. Monitoring by ^1H NMR reveals that the cycloaddition of **8b** proceeds almost quantitatively, and more smoothly than those of **8a** and **8c**. Accordingly, **8c** forms the cycloadducts **15** and **16** in a 1:2 ratio. However, simple linear 1,2-diethynyltetramethyldisilane and 1,2-diethynyltetramethyldigermane do not undergo the addition reaction with DDQ in CH_2Cl_2.

Recently, on irradiation in the presence of hexamethyldisilane and hexamethyldigermane in chloroform, some quinones were reported to give the corresponding mono- and dimetallated hydroquinones through triplet radical ion pairs generated by electron transfer [62,63]. However, the cycloaddition mechanism of the cyclic diethynylenes and DDQ is not yet clear, but is conceived to proceed via these electron donor–acceptor pairs from considerations of the appearance of the characteristic CT absorption band and the relative reactivity among these diynes. The cycloaddition above constitutes another example showing the insertion of a quinone unit into Si–Si and Ge–Ge bonds without transition metal catalysts [64,65].

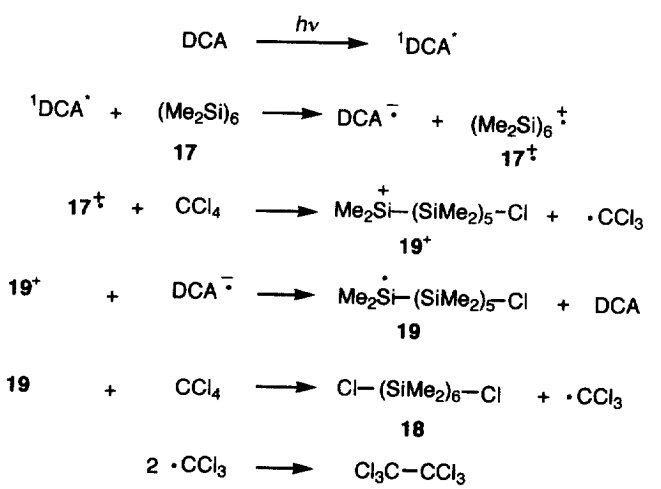

Scheme 2. Mechanism for the photo-induced chlorinative cleavage of a Si–Si σ bond.

$$(Me_2Si)_6 \xrightarrow[DCA\ /\ CCl_4\text{-}CH_2Cl_2]{h\nu\ (\lambda > 300\ nm)} Cl\text{–}(SiMe_2)_6\text{–}Cl + Cl_3C\text{–}CCl_3 \quad (7)$$

17 **18**

3. Photo-induced electron transfer reaction of organosilicon and related compounds

3.1. Photo-induced chlorinative Si–Si bond cleavage

Irradiation of dodecamethylcyclohexasilane (**17**) in a mixed solvent of CCl_4–CH_2Cl_2 in the presence of DCA resulted in the formation of 1,6-dichlorohexasilane **18** in 60–80% yields together with hexachloroethane [Eq. (7)] [5]. The reaction did not occur without DCA under these conditions, and it is clear that DCA should be excited first by light of wavelength longer than 300 nm. Furthermore, the free energy change (ΔG) from **17** to the excited singlet state of DCA ($^1DCA^*$) is calculated to be −17 kcal/mol by the Rehm–Weller equation [66]. These are the indications of exothermic electron transfer from cyclic silane **17** to $^1DCA^*$. This is substantiated by the fact that the fluorescence of DCA in CH_2Cl_2 was quenched by **17** at a diffusion-controlled rate. Linear permethylpolysilanes

$$(SiR^1R^2)_n \xrightarrow[DCA\ /\ EtOH\text{-}CH_3CN]{h\nu} EtO(SiR^1R^2Si)_nH \quad (8)$$

20 **21**

a: n = 3; $R^1 = R^2$ = t-$BuCH_2$; 47%, **b**: n = 4; $R^1 = R^2$ = i-Pr; 49%
c: n = 4; R^1 = t-Bu, R^2 = Me; 26%, **d**: n = 4; $R^1 = R^2$ = s-Bu; 56%

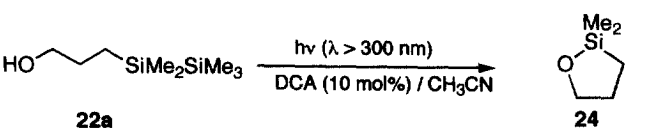

22a **24** (9)

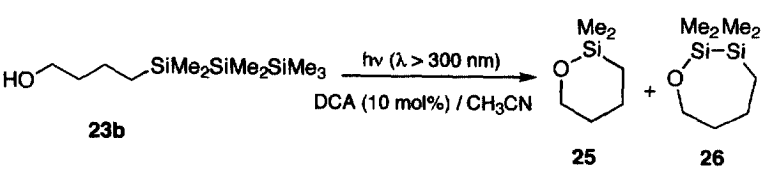

23b **25** **26**

$$HO\text{–}(CH_2)_4\text{–}(SiMe_2)_2R \quad (10)$$

23

a: R = Me, **b**: R = Me_3Si, **c**: R = C_6H_5
d: R = p-Me-C_6H_4, **e**: p-MeO-C_6H_4
f: R = p-CF_3-C_6H_4

were also chlorinatively cleaved in general under similar conditions. Thus, decamethyltetrasilane gave a mixture of 1-chloroheptamethyltrisilane, chloropentamethyldisilane, and chlorotrimethylsilane without significant regioselectivity in the Si–Si bond cleavage [34]. In this regard, the rate of the photodecomposition of poly(methylphenylsilane) has been reported to increase on addition of a halogenated sensitizer such as 1,4-bis(trichloromethyl)benzene [67]. The similar chlorinative cleavage of a Si–Si bond was effected by the treatment of polysilanes with tris(4-bromophenyl)aminium hexachloroantimonate in CH_2Cl_2 [68–70]. From these results, the reaction sequence depicted in Scheme 2 has been proposed as a possible reaction pathway for the photo-induced chlorinative Si–Si bond cleavage [5,34]. The radical nature of the key intermediate is evidenced by the formation of both chlorosilane **18** and hexachloroethane in the presence of CCl_4.

3.2. Photo-induced nucleophilic Si–Si bond cleavage

However, trapping at the cationic site of the transient intermediate by a nucleophilic solvent, such as an alcohol, is rather difficult under the reaction conditions, partly due to the extremely short lifetime of the most probable intermediate, silyl radical cation and/or rapid back-electron transfer from the DCA radical anion. In fact, nucleophilic cleavage of a polysilanyl radical cation with EtOH has been reported on highly strained cyclic polysilanes **20** with bulky substituents where the lifetime of the silyl radical cation may be lengthened by steric protection, and **20** were converted to alkoxysilanes **21** under photolysis conditions [Eq. (8)] [71].

To increase the efficiency of the nucleophilic trap, molecules containing both nucleophilic and cationic centres such as polysilanylalkanols **22** and **23** were

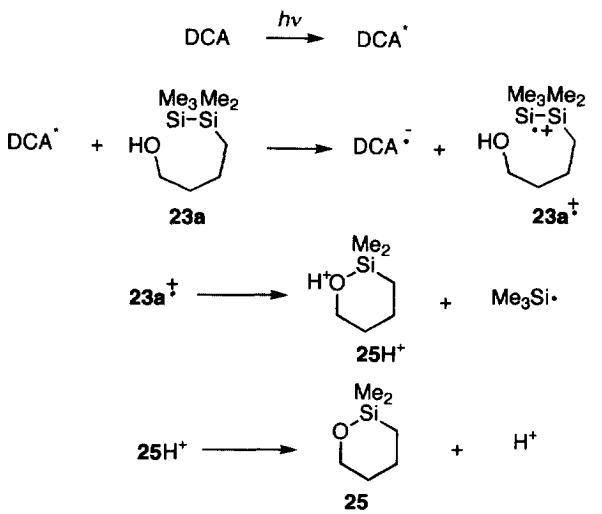

Scheme 3. Intramolecular trapping of a transient silyl radical cation with a nucleophile.

prepared. Photolysis of **22a** in CH_3CN containing a small amount of DCA with a medium pressure Hg lamp through a Pyrex filter caused cleavage of the Si–Si bond by intramolecular participation of the hydroxyl group to give cyclic silyl ether **24** [Eq. (9)] [24]. Similar photolysis of disilanylbutanol **23a** gave a six-membered cyclic silyl ether **25** (Scheme 3), but the trisilanylbutanol **23b** produced both **25** and **26** [Eq. (10)]. Similarly, DCA sensitized photoreaction of phenylpentamethyldisilanylbutanol **23c** gave silyl ether **25** in high yields together with concomitant evolution of dimethylphenylsilyl radical. Interestingly, the fate of dimethylphenylsilyl moiety was quite dependent on the reaction media. Thus, in CH_2Cl_2–CCl_4, chlorodimethylphenylsilane (91%, with **25**, 96%), in benzene, dimethyldiphenylsilane (22%, with **25**, 53%), and in EtOH–CH_3CN (1:3), ethoxydimethylphenylsilane (100%, with **25**, 100%) were obtained, respectively. These results can be accounted for from Scheme 3. Electron transfer from **23a** to $^1DCA^*$ generates the geminate radical ions composed of DCA radical anion and polysilanyl radical cation **23a**$^{+\cdot}$, in which the hydroxyl group attacks the cationic site intramolecularly to give protonated cyclic silyl ether **25H**$^+$ and trimethylsilyl radical. Deprotonation of **25H**$^+$ yields **25**. It is noteworthy that intramolecular nucleophilic trapping prevails over the intermolecular variety. Chemical evidence for the intervention of the silyl radical is provided by the photolysis of **23c** in the presence of DCA mentioned above; namely, the formation of dimethyldiphenylsilane in benzene is readily rationalized by the reaction of dimethylphenylsilyl radical with the solvent benzene [72]. This is further substantiated by the efficient formation of chlorodimethylphenylsilane on the photolysis in CH_2Cl_2–CCl_4. Chlorodimethylphenylsilane should arise from dimethylphenylsilyl radical by abstraction of a chlorine from CCl_4. On the other hand, the formation of ethoxydimethylphenylsilane is not straightforward. Since silyl radicals have been reported to have quite low IEs [73], the possibility is that the silyl radical is transformed into the silyl cation by means of electron transfer to the ground state of DCA, followed by trapping with EtOH to give ethoxydimethylphenylsilane. A similar oxidation process is assumed for the fluorinative cleavage reaction described below. Addition of the radical to CH_3CN followed by ethanolysis is another possibility.

Table 4
DCA fluorescence quenching with aryldisilylbutanols **23c–f**

Compound	k_q (10^{10} mol^{-1} s^{-1})[a]	E_{ox}[b]	ΔG (kcal mol^{-1})[c]
23e (X = p-MeO)	1.36	1.26	−21.4
23d (X = p-Me)	0.97	1.68	−11.7
23c (X = H)	0.70	1.76	−9.9
23f (X = CF_3)	0.60	1.82	−8.5

[a] Rate constants for fluorescence quenching of DCA in CH_3CN obtained by Horiba NAES-1000 time resolved fluorimeter.
[b] Oxidation peak potentials obtained by cyclic voltammetry: Pt electrode, tetrabutylammonium perchlorate in CH_3CN vs. SCE.
[c] Calculated free energy changes on electron transfer in CH_3CN [66].

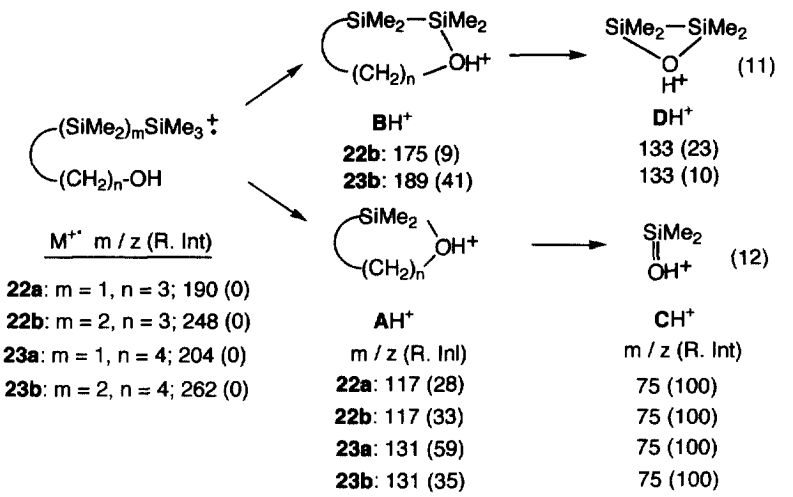

Scheme 4. Mass spectral fragmentation of polysilanylalkanols **22–23**.

The relative reaction rates among **23c–f** have been obtained by competitive photolysis in CH_3CN–MeOH containing a small amount of DCA, and the values obtained are $k_{23c}:k_{23d}:k_{23e}:k_{23f} = 1.0:1.2:1.9:0.68$. The logarithm of these relative rates against substituent constants σ^+ displays a good linear relationship, where reaction constant ρ is -0.32 ($r = 0.996$). The small but negative ρ value is consistent with the view that the Si–Si bond acts as an electron donor. The quenching rate constants of DCA fluorescence with **23c-f** also depend on the substituent on the phenyl group (Table 4). Thus, the quenching rate increases with increasing electron donating nature of substituents and vice versa. Similar trends are observed in the oxidation potentials and the calculated free energy change on electron transfer.

Polysilanylalkanols **22** and **23** showed characteristic mass spectral fragmentations as summarized in Scheme 4, which are similar to the reaction patterns of the photo-induced electron transfer reactions above [cf. Eqs. (9) and (10) and Scheme 3]. The mass spectra of **22** and **23** showed no $M^{+\cdot}$ but rather simple fragment ions. In contrast, a linear permethylpolysilane shows moderate intensity of the peak due to $M^{+\cdot}$, which eliminates a trimethylsilyl group, followed by a successive loss of a dimethylsilylene unit [74]. Thus, incorporation of the hydroxyl group altered the principal fragmentation path of the polysilanyl chain completely. The most prominent feature was the presence of peaks at m/z 117 and 131 assignable to those due

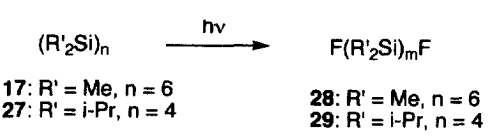

(13)

Table 5
Photo-induced fluorinative cleavage of Si–Si bonds of cyclic oligosilanes **17** and **27**

Substrate	Reaction condition[a]	Time (min)	Conv. (%)	$F(R_2Si)_mF$[b]				
				$m = 2$	3	4	5	6
17	$TPP^+BF^-_4$	10	34	15	tr	3	—	80
		20	60	20	tr	5	—	41
17	$DCA / Bu_4N^+BF^-_4$	10	13	tr	—	tr	—	35
		20	38	tr	—	tr	—	20
17	DCA/BF_3Et_2O	10	5	tr	—	tr	—	95
		60	34	tr	—	tr	—	43
27	$TPP^+BF^-_4$	10	17	—	tr	49		
		60	93	4	tr	15		
27	DCA/BF_3Et_2O	10	2	tr	—	54		
		60	30	tr	—	7		

[a] In CH_2Cl_2 and on irradiation with a tungsten–halogen lamp.
[b] tr = trace.

to AH^+. These ions decay further to give a peak at m/z 75 due to CH^+ as a base ion peak in common [Eq. (12)]. In the case of trisilanes **22b** and **23b**, there are two possible positions to be attacked by the hydroxyl group, and in addition to AH^+, a peak corresponding to BH^+ was also observed, which gave rise to the peak at m/z 133 due to DH^+ in a similar way [Eq. (11)]. The presence of both fragmentation processes, namely AH^+ to CH^+ and BH^+ to DH^+, was indicated by linked scannings (both B^2/E and B/E constant spectra) [75]. These fragmentations are readily interpreted on the basis of their chemical behaviour on photo-induced electron transfer. Thus, the cationic polysilanyl chains of **22a** and **23a** should be trapped intramolecularly by the hydroxyl group quite efficiently to give AH^+. The MS spectra of **23c–f** are very much like those of **22a** and **23a**, excepting the presence of peaks due to the corresponding phenyldimethylsilyl cation. In addition to the absence of the $M^{+\cdot}$ peak, an AH^+ and a CH^+ ion were presented as a prominent and a base peak, respectively.

3.3. Fluorinative Si–Si bond cleavage via electron transfer

Peralkylated oligosilanes are effective electron donors, and undergo chlorinative cleavage reaction of Si–Si σ bonds in CCl_4 solutions initiated by photo-induced electron transfer as described [5]. Recently, Si–Si σ bonds of oligosilanes and

$$\underset{\textbf{30}}{R_{3-n}Me_nSi\text{-}SiMe_nR'_{3-n}} \xrightarrow{h\nu} R_{3-n}Me_nSiF + FSiMe_nR'_{3-n}$$

a; R = R' = Ph, n = 1, **b**; R = R' = Ph, n = 2
c; R = $PhCH_2$, R' = Me, n = 2, **d**; R = Me_3Si, R' = Me, n = 2 (14)

Table 6
Photo-induced fluorinative cleavage of phenyldisilanes **30a** and **30b**, benzyldisilane **30c** and trisilane **30d**

Substrate	Reaction condition[a]	Time (min)	Conv. (%)	Product and yield (%)	
30a	$TPP^+BF_4^-$ [b]	60	84	Ph_2MeSiF (100)	
30a	DCA / $Bu_4N^+BF_4^-$ [c]	60	58	Ph_2MeSiF (52)	
30b	$TPP^+BF_4^-$ [b]	30	72	$PhMe_2SiF$ (100)	
30b	DCA / $Bu_4N^+BF_4^-$ [c]	240	50	$PhMe_2SiF$ (85)	
30c	$TPP^+BF_4^-$ [d]	30	61	$PhCH_2Me_2SiF$ (53)	Me_3SiF [e]
30c	DCA / $Bu_4N^+BF_4^-$ [c]	120	33	$PhCH_2Me_2SiF$ (22)	Me_3SiF [e]
30d	$TPP^+BF_4^-$ [d]	30	55	$Me_3SiSiMe_2F$ (58)	Me_3SiF [e]
30d	DCA / $Bu_4N^+BF_4^-$ [c]	120	49	$Me_3SiSiMe_2F$ (55)	Me_3SiF [e]

[a] On irradiation with a tungsten–halogen lamp.
[b] In a mixed solvent of CH_3CN and CH_2Cl_2.
[c] In CH_2Cl_2.
[d] In CH_3CN.
[e] Yield not determined.

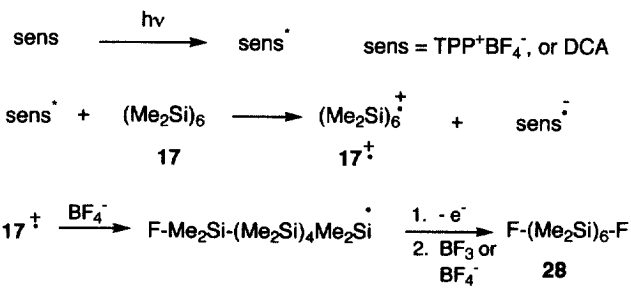

Scheme 5. Reaction mechanism for the fluorinative Si–Si bond cleavage.

phenyldisilanes have been shown to be subjected also to fluorinative cleavage via photo-induced electron transfer [76].

Irradiation of cyclic silanes **17** and **27** in CH_2Cl_2 in the presence of 2,4,6-triphenylpyrylium tetrafluoroborate ($TTP^+BF_4^-$) with tungsten–halogen lamps causes fluorinative Si–Si bond cleavage and gives the corresponding α,ω-difluorohexasilanes **28** and **29** as main products [Eq. (13)]. Prolonged irradiation results in further fluorinative cleavage of the product formed to give difluorodisilane and difluorotetrasilane as shown in Table 5. Recently, electrochemical oxidation of cyclic peralkylsilanes using n-$Bu_4N^+BF_4^-$ as supporting electrolyte has been reported to undergo Si–Si bond cleavage reaction with tetrafluoroborate anion to form α,ω-difluorosilanes [77]. The photo-induced cleavage reaction does not proceed without light and pyrylium salt, and is inhibited by the addition of 1,4-diazabicyclo[2.2.2]octane [DABCO, oxidation potential (E_{ox}) +0.70 V vs. SCE]. ΔG values estimated from the Rehm–Weller equation indicate exothermic electron transfer from polysilanes **17** and **27** to the excited singlet state of the sensitizer (ΔG: $Bu_4N^+BF_4^-$; **17**, −21.9 kcal/mol; **27**, −31.4 kcal/mol) [66]. The fluorescence of the pyrylium salt is

efficiently quenched with the polysilanes ($k_q\tau$: **17**, 140 M^{-1}; **27**, 160 M^{-1}). The sensitized irradiation of **17** and **27** with DCA in the presence of tetrabutylammonium tetrafluoroborate ($Bu_4N^+BF_4^-$) also gives the corresponding α,ω-difluorooligosilanes. Fluorination occurs even in the absence of the tetrafluoroborate, namely difluorosilanes are produced on irradiation of **17** and **27** in the presence of DCA and trifluoroborane etherate ($BF_3 \cdot Et_2O$). Octaisopropylcyclotetrasilane (**27**) undergoes a similar photo-induced fluorinative cleavage reaction to give the corresponding difluorosilanes. The results obtained so far are summarized in Table 5. Upon irradiation in the presence of TTP^+BF_4, 1,2-dimethyltetraphenyldisilane (**30a**), 1,2-diphenyltetramethyldisilane (**30b**), benzylpentamethyldisilane (**30c**), and octamethyltrisilane (**30d**) underwent a fluorinative Si–Si bond cleavage reaction to yield the corresponding fluorosilanes in reasonable yields [Table 6 and Eq. (14)]. Furthermore, under these reaction conditions hexamethyldisilane also converted to give fluorotrimethylsilane.

An account of these fluorinative cleavage reactions is shown in Scheme 5 using **17** as an example. Similar to the chlorinative cleavage, the first step of the reaction should be one-electron transfer from organosilane **17** to the excited singlet state of the sensitizer (TPP^+BF_4 and DCA) to form a radical ion pair, namely radical cation $\mathbf{17}^{+\cdot}$ and the radical anion of the sensitizer. This is substantiated by negative ΔG values, and efficient quenching of the fluorescence of sensitizers. Then, the nucleophilic attack of BF_4^- on $\mathbf{17}^{+\cdot}$ causes Si–Si bond fission to give difluorosilane **28** followed by oxidation and another fluorination possibly by BF_4^- or BF_3.

3.4. Skeletal rearrangement via photo-induced electron transfer

Direct irradiation of silanorbornadiene **6** with a medium pressure Hg arc lamp in the presence of a silylene trapping reagent gives skeletal rearranged products **31** and **32** accompanied by anthracene and the corresponding silylene adduct **33** [Eq. (15)] [44]. Effective $\sigma-\pi$ conjugation between the benzene π-system and the Si–C σ bonds causes silanorbornadiene **6** to form a CT complex with TCNE as mentioned above. Therefore, it is of particular interest to examine if such a rearrangement also takes place under photo-induced electron transfer conditions. Thus, irradiation of a solution of **6** and DCA in degassed dry CH_2Cl_2 with two

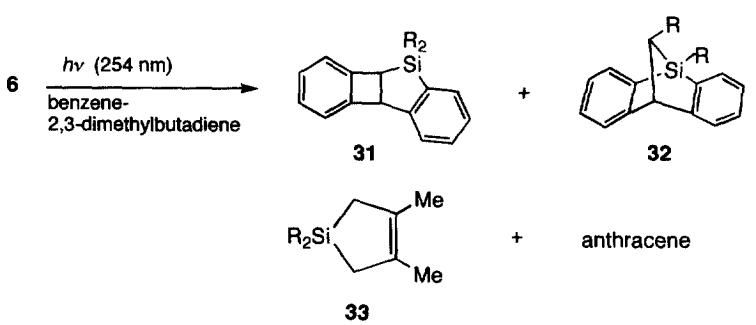

(15)

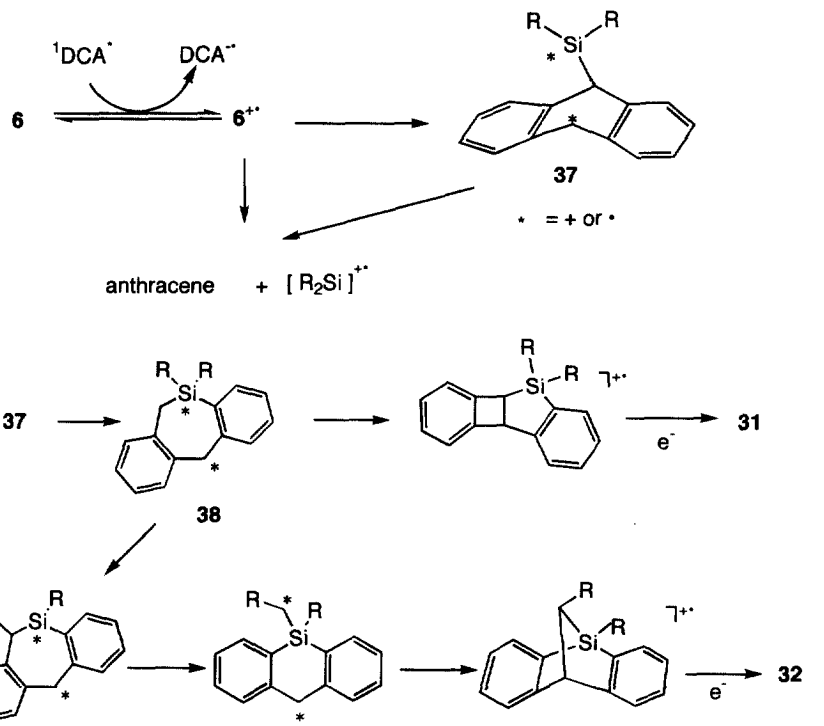

Scheme 6. Mechanism for the skeletal rearrangement via electron transfer.

tungsten–halogen lamps (passing through an aqueous $NaNO_2$ solution filter, cut-off < 400 nm) gave the same rearranged products **31** and **32** together with anthracene, 31% and 36% yields, respectively [78]. The photoreaction of **6** occurred also in CH_3CN but proceeded slowly in benzene. No reaction took place when **6** was irradiated with a longer wavelength light (> 400 nm) in the absence of the sensitizer. Meanwhile, addition of DABCO, which has a lower oxidation potential than that of **6** (E_{ox} = +1.40 V vs. SCE), suppressed the consumption of **6**. A ΔG value of −12.9 kcal/mol indicates an exothermic electron transfer from **6** to $^1DCA^*$. The fluorescence of DCA was efficiently quenched with **6** ($k_q = 7.9 \times 10^9\ M^{-1}\ s^{-1}$). On the other hand, neither exciplex emission nor CT absorption

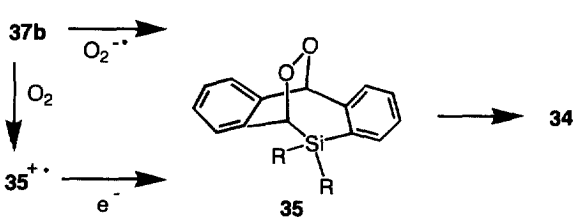

Scheme 7. Photo-oxygenation of **6a** in the presence of the sensitizer.

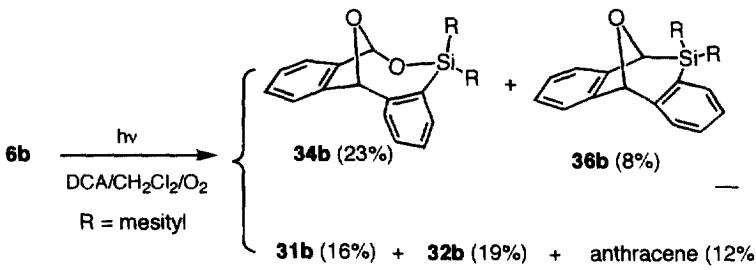

(16)

was observed between **6** and DCA. So, the photorearrangement in the presence of the sensitizer would be reasonably accounted for by a stepwise process induced by initial electron transfer from **6** to $^1DCA^*$ outlined in Scheme 6.

Probably, electron transfer occurs from the bridge C–Si bond to form a radical cation $6^{+\cdot}$. Then, $6^{+\cdot}$ would collapse to give **37** by C–Si bond cleavage, and isomerize to another open key intermediate **38** by migration of one of the aromatic groups. Ring-closure and subsequent back-electron transfer leads to **31**. Meanwhile, the formation of **32** would be accounted for by the two-fold 1,2-migration of two aromatic groups followed by ring-closure and back-electron transfer. In these reduction steps, $DCA^{-\cdot}$ or neutral **6** probably serves as the electron source. Formation of anthracene in substantial yields in all the reaction conditions employed suggests that the second C–Si bond cleavage in **37** or spontaneous extrusion of the R_2Si moiety from $6^{+\cdot}$ would occur. However, no product derived from the eliminated R_2Si moiety was detected even in the presence of 2,3-dimethyl-1,3-butadiene, which is an efficient trapping reagent for silylene.

To obtain further insight into the rearrangement mechanism, **6b** was photolyzed in the presence of molecular oxygen, which has been reported to trap various radical cations efficiently [21,22,79–84] (for a recent review, see ref. [85]). When

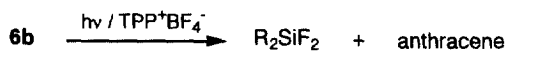

(17)

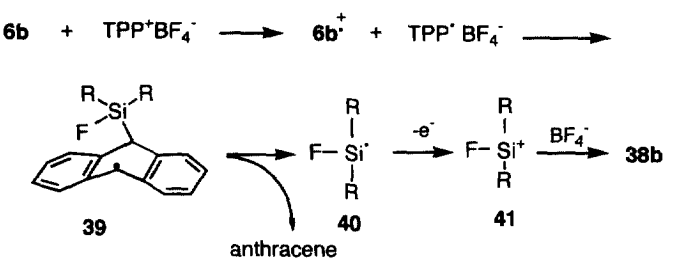

Scheme 8. Plausible reaction pathway for photo-induced fluorination of **6b**.

DCA-sensitized photolysis of **6b** was carried out under bubbling oxygen, an oxygen adduct **34b** (23%) was obtained while the yields of **31b** and **32b** were decreased (16% and 19%, respectively) [Eq. (16)]. With careful analysis of spectral data, the structure of the oxygen adduct was assigned to **34b** instead of endoperoxide **35**, since it was thermally stable and could not be reduced by Ph_3P. It was confirmed that **31** and **32** were inert under the oxygenation conditions. Therefore, it is likely that the intermediate **38** is trapped by $O_2^{-\cdot}$ giving **35**, which would be unstable and undergo isomerization via the O–O bond cleavage. It should be noted that, as another route, **35** could be formed by O_2 addition to **37b** followed by reduction (Scheme 7). To our knowledge, the isomerization described here represents the first example of photosensitized skeletal rearrangement of organosilicon compounds.

When a CH_2Cl_2 solution of **6b** in the presence of $TPP^+BF_4^-$ was irradiated with 500 W tungsten–halogen lamps (passing through an aqueous $NaNO_2$ solution filter, cut-off < 400 nm), **6b** was rapidly consumed and anthracene and difluorodimesitylsilane (**38b**) were obtained in 89% and 59%, respectively [Eq. (17)]. The fluorescence of $TPP^+BF_4^-$ was efficiently quenched with **6b** ($k_q\tau = 70\ M^{-1}$), and the ΔG of electron transfer process between **6b** and $TPP^+BF_4^-$ is calculated to be −29.9 kcal/mol, which suggests an exothermic electron transfer from **6b** to the excited singlet state of $TPP^+BF_4^-$. The reaction did not occur without the sensitizer or under dark conditions, and was suppressed by addition of electron donors such as DABCO. On the other hand, neither exciplex emission nor CT absorption was observed between **6b** and the acceptors ($TPP^+BF_4^-$ and DCA). These reactions can be accounted for by a process induced by initial electron transfer from **6b** to the acceptors.

A plausible reaction mechanism for **6b** is shown in Scheme 8. Initially, the bridge Si–C bond would be oxidized and cleaved by a nucleophilic attack of BF_4^- to form an open intermediate **39**, which may subsequently release neutral anthracene and fluorosilyl radical **40**. Since the IE of a silyl radical has been reported to be quite low [73], **40** might undergo further one-electron oxidation to give silyl cation **41**, which should react with BF_4^- as a F^- source to produce difluorosilane **38b**.

Table 7
Photo-induced fluorination of silanorbornadiene **6b**

Substrate	Reaction condition[a]	Time (h)	Conv. (%)	Product and yield (%)				
				31	**32**	**An**[b]	**38b**	**Ad**[c]
6b	$TPP^+BF^-_4$	2	100	0	0	89	59	
6b	DCA / $Bu_4N^+BF^-_4$	3	78	18	18	36	14	
6b	DCA	3	89	31	36	18	0	
6b	TCNE / $Bu_4N^+BF^-_4$	3	85	18	18	0	14	36

[a] On irradiation with a tungsten–halogen lamp in CH_2Cl_2.
[b] **An**: anthracene.
[c] **Ad**: the cycloaddition product of anthracene and TCNE.

In the TPP$^{+}BF_4^{-}$ sensitized reaction of **6b**, neither **31b** or **32b** was detected, in contrast to the case of the DCA sensitization, which suggests that the fluorinative cleavage reaction should occur at an early stage, before the rearrangement in the total reaction pathway. The Si–F bonds have large bond formation energies, so fluoride ions might be transferred quite rapidly from BF_4^{-} to silyl radical cation **6b**$^{+\cdot}$ and eventually furnish **38b**. In fact, **38b** was readily produced when DCA-sensitized photoreaction of **6b** was carried out in the presence of n-$Bu_4N^{+}BF_4^{-}$, whereas production of the rearrangement products, **28b** and **32b**, was suppressed. Under the same conditions, **31b** was confirmed to be stable and **32b** was found to be photoreactive, but produced neither anthracene nor **38b**. Since TCNE is also known as a strong acceptor to oxidize various donors, a CH_2Cl_2 solution of **6b** and TCNE was photolyzed in the presence of n-$Bu_4N^{+}BF_4^{-}$ with visible light. As

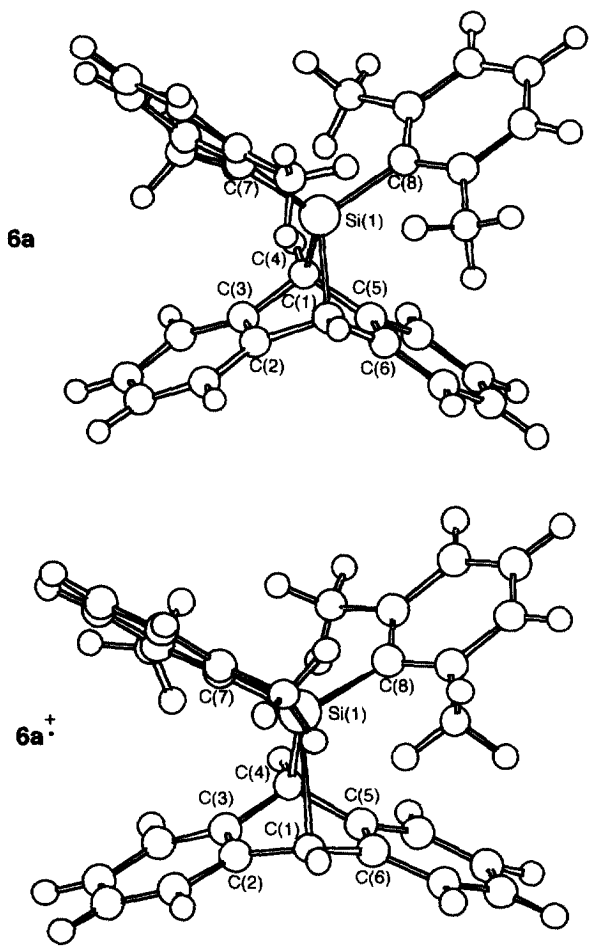

Fig. 1. MOPACPM3 optimized structures for **6a** and **6a**$^{+\cdot}$.

Table 8
Selected bond distances (Å) and angles (°) of **6a** and **6a**$^{+\cdot}$

	X-ray data	Calculated data[a]	
	6a	**6a**	**6a**$^{+\cdot}$
Si(1)–C(1)	1.944(5)	2.024	2.599
Si(1)–C(4)	1.930(5)	2.026	1.983
Si(1)–C(7)	1.905(5)	1.875	1.821
Si(1)–C(8)	1.886(5)	1.878	1.835
C(1)–C(2)	1.527(7)	1.491	1.433
C(1)–C(6)	1.509(7)	1.491	1.434
C(1)–Si(1)–C(4)	80.4(2)	78.379	70.752
C(1)–Si(1)–C(7)	112.3(2)	111.543	104.552
C(1)–Si(1)–C(8)	117.9(2)	119.713	114.344
C(4)–Si(1)–C(7)	119.2(2)	117.881	123.273
C(4)–Si(1)–C(8)	110.5(2)	114.132	114.917
C(7)–Si(1)–C(8)	113.0(2)	111.715	117.580
Si(1)–C(1)–C(6)	97.8(3)	96.418	82.076
Si(1)–C(1)–C(2)	97.0(3)	95.637	83.154
C(6)–C(1)–C(2)	107.4(4)	107.362	117.662
Si(1)–C(4)–C(5)	96.4(3)	96.485	97.047
Si(1)–C(4)–C(3)	97.1(3)	96.233	99.124
C(5)–C(4)–C(3)	107.6(4)	107.663	111.146

[a] Calculated by MOPAC PM3 [51,52].

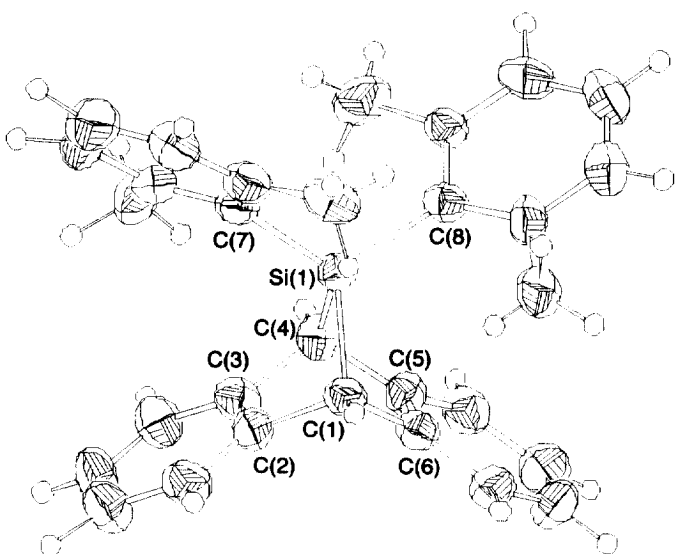

Fig. 2. Molecular structure of **6a** in the crystals: ORTEP drawing and numbering scheme.

Table 9
Ionization energies (IE) of **6a,b** and some benzylic silanes

Silane	EI (eV)[a]
$Me_3SiCH_2C_6H_5$	8.06 (8.35)
1,2-$(Me_3SiCH_2)_2C_6H_4$	7.71 (8.05)
1,4-$(Me_3SiCH_2)_2C_6H_4$	7.63 (7.75)
1,2,4,5-$(Me_3SiCH_2)_4C6H_2$	7.01 (7.10)
6a	7.42
6b	7.36

[a] Experimental values are in parentheses.

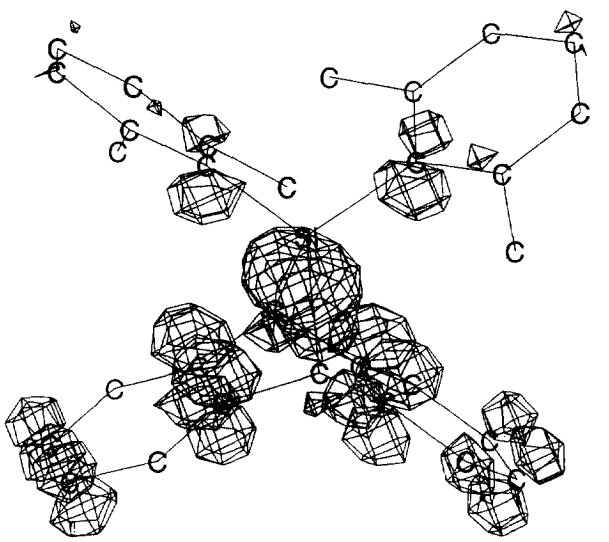

Fig. 3. Calculated HOMO orbital for **6a**.

expected, **6b** was readily consumed to give **38b** along with the Diels–Alder adduct of anthracene and TCNE as shown in Table 7.

3.5. The structure of a silyl radical cation

In recent times, the chemistry of a free silyl cation has been argued intensively from experimental and theoretical points of views [86–88]. Since silicon is more positive than carbon, the silyl cation should be more thermodynamically stable than its carbon analogue. In spite of the fact that the trivalent silyl cation is readily formed in the vapour phase, such as in an ion chamber of a mass spectrometer [89], this is not true in condensed phases; the silyl cation is extremely sensitive towards Lewis bases and is coordinated even with toluene and a carbon–carbon double bond [90,91]. After many attempts to isolate the free silyl cation in condensed

Table 10
Charge and spin density of radical cation **6a**$^{+\cdot}$

Atom	Charge	(ΔCharge[a])	Spin density
Si(1)	+0.905	(+0.443)	+0.200
C(1)	−0.072	(−0.006)	−0.154
C(2)	−0.062	(−0.001)	+0.467
C(3)	−0.073	(−0.018)	−0.417
C(4)	−0.058	(+0.029)	+0.633
C(5)	−0.069	(−0.018)	−0.425
C(6)	−0.061	(+0.001)	+0.499
C(7)	−0.257	(−0.063)	−0.155
C(8)	−0.264	(−0.067)	−0.111
Fragment	Charge	(ΔCharge[a])	Spin density
Si atom	+0.904	(+0.443)	+0.200
2.6-Dimethylphenyl	−0.134	(+0.178)	+0.022
Anthracene	+0.229	(+0.379)	+0.778

[a] Change of the charge from neutral **6a** to cation radical **6a**$^{+\cdot}$.

phases, finally $[(mesityl)_3Si]^+[B(C_6F_5)_4]^-$ has been prepared and its spectroscopic data are reasonably interpreted by no interaction with an aromatic solvent [92]. On the other hand, since a silyl radical cation should have both radical and cationic characters, a silyl radical cation is adequately thought to be more reactive than the corresponding silyl cation. In fact, a silyl cation radical is hardly trapped intermolecularly by an alcohol without sterically crowded substituents on the cationic silicon centre [5,24,25,29,34]. Studies on silyl cations may lead to isolation of the elusive silyl radical cation in the near future. A limited number of structural studies on the silicon centred cation radical have been reported so far [93–97], therefore we have examined the structure of newly generated silyl radical cation **6a**$^{+\cdot}$ in some detail.

In addition to the efficient fluorescence quenching of the sensitizer and exothermic electron transfer from the σ-donor to the excited singlet state of the sensitizer estimated by the Rehm–Weller equation [66], the radical cationic nature of the key intermediate is evidenced experimentally by Eqs. (7),(9),(10). Now, to reveal the structure of the so far elusive key intermediate silyl radical cation, an investigation by combination of X-ray crystallographic analysis and MOPAC calculation has been done.

The optimized structure of **6a** and the corresponding radical cation **6a**$^{+\cdot}$ are

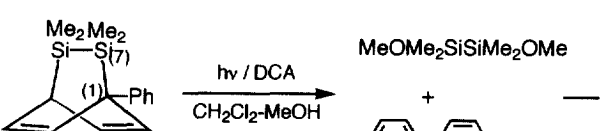

42

(18)

calculated by the MOPAC PM3 method [51,52], as shown in Fig. 1 with selected geometrical parameters in Table 8. To verify the validity of the calculation, the structure of **6a** in crystals was determined by X-ray crystallographic analysis. The molecular structure of **6a** is shown with important bond lengths and angles in Fig. 2 and Table 8. The bond lengths and angles are fairly close to those reported for related silanorbornadiene derivatives [98–100]. The bridge Si–C bonds are slightly longer than normal Si–C bonds [101]. Similar bond elongation in the silanorbornadiene skeleton was reported and explained in terms of delocalization of electron density of the bridge Si–C σ bond to the π bonds of the anthracene moiety [100]. The validity of the optimized structure of **6a** was thus supported by a comparison with that obtained by the X-ray analysis. Adiabatic ionization energies (IE) of **6a,b** were also estimated to be 7.42 and 7.36 eV, respectively, by calculating the gap of heats of formation between the neutral and the radical cation. As shown in Table 9, these values are reasonable since the calculated IE values for bis- and tetrakis-Me_3SiCH_2 benzenes as related compounds show good consistency with those measured by photoelectron spectroscopy [102]. The calculated HOMO drawing of **6a** is illustrated in Fig. 3. The HOMO has surely delocalized both the aromatic π systems and the benzylic C–Si bond.

Some characteristics of the radical cation $\mathbf{6a}^{+\cdot}$ were carefully examined to gain insight into the reaction mechanism. The most important structural features of $\mathbf{6a}^{+\cdot}$ are as follows: (i) one bridge Si–C bond [Si(1)–C(1), 2.60 Å] much longer compared with the other one [Si(1)–C(4), 1.98 Å] and those of neutral **6a** [Si(1)–C(1), 2.02 Å; Si(1)–C(4), 2.03 Å]; (ii) marked flattening of the Si(1) atom and the C(1) atom [the sum of angles C(7)–Si(1)–C(8), C(4)–Si(1)–C(7) and C(4)–Si(1)–C(8) being 355.8°, and C(2)–C(1)–C(6), C(2)–C(1)–H(1) and C(6)–C(1)–H(1) 356.49°]; (iii) slight but appreciable shortening of Si(1)–C(4), Si(1)–C(7), Si(1)–C(8), C(1)–C(2), and C(1)–C(6) bonds on the transformation from **6a** to $\mathbf{6a}^{+\cdot}$. Some electronic properties of the optimized radical cation are summarized in Table 10. A significant population of the positive charge is observed at the Si(1) atom, whereas the spin population is more predominant at the anthracene unit than at the silicon atom and the 2,6-dimethylphenyl group as shown. Therefore, it is suggested that the Si(1)–C(1) bond of $\mathbf{6a}^{+\cdot}$ has a tendency to dissociate as a cationic silyl site and a diarylmethyl radical site. Similar structural and electronic aspects were reported for the radical cation $[t\text{-}Bu_3SiH]^{+\cdot}$ calculated from the MOPAC AM1 method [51,52,96,97].

In addition to the HOMO of **6a**, these findings described above indicate that one electron is removed from one of the bridge C bonds, which would be weakened subsequently to the relaxed form of $\mathbf{6a}^{+\cdot}$ as depicted in Fig. 1. The presence of nucleophiles such as alcohol and fluoride ion should accelerate the cleavage of the Si–C bond.

DCA sensitized irradiation in CH_2Cl_2–MeOH, 1-phenyl-7,7,8,8-tetramethyl-7,8-disilabicyclo[2.2.2]octa-2,5-diene (**42**) was readily photolyzed to give 1,2-dimethoxytetramethyldisilane and biphenyl as expected [Eq. (18)] [103–106]. The structure of silyl radical cation $\mathbf{42}^{+\cdot}$ was also studied by ab initio MO calculation (RHF/3-21*) of the parent compound, 7,8-disilabicyclo[2.2.2]octa-2,5-diene, and showed similar electronic and geometrical characteristics to those of $\mathbf{6a}^{+\cdot}$, namely elongation of

one of the two Si–C(allylic) bonds [C(1)–Si(7)] and marked flattening of the Si(7) and C(1) centers. Together with the stereochemistry of the Si–C bond cleavage, the detailed reaction mechanism is under investigation.

Acknowledgements

We appreciate the efforts of our coworkers, whose names appear in the references. Special thanks go to Professor Hideki Sakurai for his invaluable stimulation and encouragement. We also thank the Ministry of Education, Science, Sports, and Culture, Japan for financial support (Grants-in-Aid for Scientific Research on Priority Areas No. 0623922, 06227226 and 09239215, and for Encouragement for Young Scientists No. 06854031).

References

[1] J.Y. Corey, in: S. Patai, Z. Rappoport (Eds.), The Chemistry of Organic Silicon Compounds, Wiley, Chichester, UK, 1989, chapter 1, p. 1.
[2] H. Bock, H. Alt, J. Am. Chem. Soc. 92 (1970) 1569.
[3] H. Bock, Angew. Chem., Int. Ed. Engl. 28 (1989) 1627.
[4] H. Sakurai, K. Sakamoto, M. Kira, Chem. Lett. (1984) 1213.
[5] Y. Nakadaira, N. Komatsu, H. Sakurai, Chem. Lett. (1985) 1781.
[6] S. Kyushin, Y. Ehara, Y. Nakadaira, M. Ohashi, J. Chem. Soc., Chem. Commun. (1989) 279.
[7] S. Kyushin, Y. Masuda, K. Matsushita, Y. Nakadaira, M. Ohashi, Tetrahedron Lett. 31 (1990) 6395.
[8] Y. Nakadaira, Y. Ohkura, S. Kyushin, M. Ohashi, K. Ueno, S. Kanouchi, H. Sakurai, Tetrahedron Lett. 33 (1992) 4013.
[9] S. Kyushin, Y. Ohkura, Y. Nakadaira, M. Ohashi, M. Yasui, F. Iwasaki, Chem. Lett. (1991) 883.
[10] S. Kyushin, Y. Baba, Y. Nakadaira, M. Ohashi, Main Group Metal Chem. 18 (1995) 299 and references cited therein
[11] K. Nakanishi, K. Mizuno, Y. Otsuji, Bull. Chem. Soc. Jpn. 66 (1993) 2371.
[12] T. Tamai, K. Mizuno, I. Hashida, Y. Otsuji, Bull. Chem. Soc. Jpn. 66 (1993) 3747.
[13] K. Mizuno, K. Nakanishi, J. Chosa, Y. Otsuji, J. Organomet. Chem. 473 (1994) 35.
[14] U.C. Yoon, P.S. Mariano, Acc. Chem. Res. 25 (1992) 233.
[15] M. Fagnoni, M. Mella, A. Albini, Tetrahedron 50 (1994) 6401.
[16] M. Mella, E. Fusan, A. Albini, J. Org. Chem. 57 (1992) 6210.
[17] X. Zhang, S.-R. Yeh, S. Hong, M. Freccero, A. Albini, D.E. Falvey, P.S. Mariano, J. Am. Chem. Soc. 116 (1994) 4211 and references cited therein
[18] S. Fukuzumi, T. Kitano, K. Mochida, J. Am. Chem. Soc. 112 (1990) 3246.
[19] S. Fukuzumi, T. Kitano, K. Mochida, J. Chem. Soc., Chem. Commun. (1989) 279.
[20] H. Sakurai, K. Sakamoto, M. Kira, Chem. Lett. (1989) 2177 and references cited therein.
[21] T. Akasaka, K. Sato, M. Kako, W. Ando, Tetrahedron Lett. 32 (1991) 6605.
[22] T. Akasaka, K. Sato, M. Kako, W. Ando, Tetrahedron 48 (1992) 3283.
[23] W. Ando, M. Kako, T. Akasaka, Chem. Lett. (1993) 1679 and references cited therein.
[24] Y. Nakadaira, A. Sekiguchi, Y. Funada, H. Sakurai, Chem. Lett. (1991) 327.
[25] Y. Nakadaira, S. Otani, S. Kyushin, M. Ohashi, H. Sakurai, Y. Funada, K. Sakamoto, A. Sekiguchi, Chem. Lett. (1991) 601.
[26] J.P. Dinnocenzo, S. Farid, J.L. Goodman, I.R. Gould, W.P. Todd, S.L. Mattes, J. Am. Chem. Soc. 111 (1989) 8973.
[27] W.P. Todd, J.P. Dinnocenzo, J.L. Goodman, I.R. Gould, Tetrahedron Lett. 34 (1993) 2863.

[28] J.P. Dinnocenzo, S. Farid, J.L. Goodman, I.R. Gould, W.P. Todd, Mol. Cryst. Liq. Cryst. 194 (1991) 151.
[29] H. Watanabe, M. Kato, E. Tabei, H. Kuwabara, N. Hirai, T. Sato, Y. Nagai, J. Chem. Soc., Chem. Commun. (1986) 1662 and references cited therein.
[30] G.J. Kavarnos, N.J. Turro, Chem. Rev. 86 (1986) 401.
[31] M.A. Fox, M. Chanon (Eds.), Photo-induced Electron Transfer, Elsevier, Amsterdam, 1988, Part A.
[32] M.G. Steinmetz, Chem. Rev. 95 (1995) 1527.
[33] G.J. Kavarnos, Fundamentals of Photoinduced Electron Transfer, VCH, New York, 1993.
[34] Y. Nakadaira, S. Kyushin, M. Ohashi, J. Synth. Org. Chem. Jpn. 48 (1990) 331.
[35] M. Kako, T. Morita, T. Torihara, Y. Nakadaira, J. Chem. Soc., Chem. Commun. 678 (1993).
[36] Y. Nakadaira, M. Kawasaki, D.-Y. Zhou. M. Kako, Main Group Metal Chem. 17 (1994) 553.
[37] S. Kyushin, Y. Nakadaira, M. Ohashi, Chem. Lett. (1990) 2191.
[38] S. Kyushin, S. Otani, T. Takahashi, Y. Nakadaira, M. Ohashi, Chem. Lett. (1991) 775.
[39] G. Briegleb, Elektron–Donator–Acceptor-Komplexe, Springer-Verlag, Berlin, 1961.
[40] R. Foster, Organic Charge-transfer Complexes, Academic Press, New York, 1969.
[41] V.F. Traven, R. West, J. Am. Chem. Soc. 95 (1973) 6824.
[42] H. Sakurai, M. Kira, T. Uchida, J. Am. Chem. Soc. 95 (1973) 6826.
[43] H. Sakurai, K. Sakamato, M. Kira, Chem. Lett. (1984) 1213.
[44] H. Sakurai, K. Oharu, Y. Nakadaira, Chem. Lett. (1986) 1797.
[45] R.S. Mulliken, J. Am. Chem. Soc. 74 (1952) 811.
[46] Y. Nakadaira, Y. Gomi, H. Hosoe, S. Kyushin, M. Kako, K. Hatakenaka, M. Ohashi, Bull. Chem. Soc. Jpn. 66 (1993) 344.
[47] M. Kako, S. Kakuma, K. Hatakenaka, Y. Nakadaira, M. Yasui, F. Iwasaki, Tetrahedron Lett. 36 (1995) 6293.
[48] S. Kyushin, Y. Izumi, S. Tsunakawa, H. Matsumoto, Chem. Lett. (1992) 1393.
[49] S. Kyushin, M. Ikarugi, S. Tsunakawa, Y. Izumi, M. Miyake, H. Matsumoto, M. Goto, J. Organomet. Chem. 473 (1994) 19.
[50] S. Kyushin, M. Ikarugi, K. Takatsuna, M. Goto, H. Matsumoto, J. Organomet. Chem. 510 (1996) 121.
[51] J.J.P. Stewart, Comput. Chem. 10 (1989) 209.
[52] J.J.P. Stewart, QCPE Bull. 9 (1989) 10.
[53] H. Sakurai, Y. Nakadaira, A. Hosomi, Y. Eriyama, C. Kabuto, J. Am. Chem. Soc. 105 (1983) 3359.
[54] K. Morokuma, in: H. Sakurai (Ed.), Organosilicon and Bioorganosilicon Chemistry, Ellis Horwood, Chichester, UK, 1985, chapter 4.
[55] R. Gleiter, Angew. Chem., Int. Ed. Engl. 31 (1992) 27.
[56] H. Komoriya, M. Kako, Y. Nakadaira, K. Mochida, M. Tonogaki-Kubota, T. Kobayashi, Chem. Lett. (1994) 1439.
[57] H. Komoriya, M. Kako, Y. Nakadaira, K. Mochida, M. Tonogaki-Kubota, T. Kobayashi, J. Organomet. Chem. 499 (1995) 123.
[58] K. Mochida, S. Masuda, Y. Harada, Chem. Lett. (1992) 2281.
[59] K. Mochida, C. Hodota, R. Hata, S. Fukuzumi, Organometallics 12 (1993) 586.
[60] K. Mochida, R. Hata, C. Hodota, S. Fukuzumi, M. Kako, Y. Nakadaira, Chem. Lett. (1995) 245.
[61] J.P. Dinnocenzo, S. Farid, J.L. Goodman, I.R. Gould, W.P. Todd, S.L. Mattes, J. Am. Chem. Soc. 111 (1989) 8973.
[62] M. Igarashi, T. Ueda, M. Wakasa, Y. Sakaguchi, H. Hayashi, J. Organomet. Chem. 421 (1991) 9.
[63] M. Wakasa, M. Igarashi, Y. Sekiguchi, H. Hayashi, Nihonkagakukaishi (1994) 267.
[64] K. Tamao, S. Okazaki, M. Kumada, J. Organomet. Chem. 146 (1978) 87.
[65] N.P. Reddy, H. Yamashita, M. Tanaka, J. Organomet. Chem. 114 (1992) 6596.
[66] D. Rehm, A. Weller, Isr. J. Chem. 8 (1970) 259.
[67] M. Stolka, H.-J. Yuh, K. McGrane, D.M. Pai, J. Polym. Sci. Part A: Polym. Chem. 25 (1987) 823.
[68] W. Shmidt, E. Steckham, Chem. Ber. 113 (1980) 577.
[69] N.L. Bauld, D.J. Bellville, B. Harrichian, K.T. Lorenzer, R.A. Pabon, Jr., D.W. Reynolds, D.D. Wirth, H.-S. Chiou, B.K. Marsh, Acc. Chem. Res. 20 (1987) 371.

[70] Y. Funada, Ms. Dissertation, Tohoku University, 1988.
[71] H. Watanabe, M. Kato, E. Tabei, H. Kuwabara, N. Hirai, T. Sato, Y. Nagai, J. Chem. Soc., Chem. Commun. (1986) 1662.
[72] M. Kira, H. Sugiyama, H. Sakurai, J. Am. Chem. Soc. 105 (1983) 6436.
[73] C. Chatgilialoglu, Chem. Rev. 59 (1995) 1229.
[74] Y. Nakadaira, Y. Kobayashi, H. Sakurai, J. Organomet. Chem. 63 (1973) 79.
[75] K.R. Jennings, R.S. Mason, in: F.W. McLafferty (Ed.), Tandem Mass Spectrometry, Wiley, New York, 1983, chapter 9, p. 197.
[76] M. Kako, K. Hatakenaka, Y. Nakadaira, unpublished results, 1997.
[77] J.Y. Becker, E. Shakkour, R. West, Tetrahedron Lett. 33 (1992) 5633.
[78] M. Kako, S. Kakuma, K. Hatakenaka, Y. Nakadaira, M. Yasui, F. Iwasaki, Tetrahedron Lett. 36 (1995) 6293.
[79] J. Eriksen, C.S. Foote, J. Am. Chem. Soc. 102 (1980) 6083.
[80] J. Steichen, C.S. Foote, J. Am. Chem. Soc. 103 (1981) 1855.
[81] C.S. Foote, Tetrahedron 41 (1985) 2221.
[82] S.F. Nelsen, Acc. Chem. Res. 20 (1987) 369.
[83] K. Mizuno, N. Kamiyama, N. Ichinose, Y. Otsuji, Tetrahedron 41 (1985) 2207.
[84] T. Miyashi, M. Kamata, T. Mukai, J. Am. Chem. Soc. 109 (1987) 2780 and references cited therein
[85] M.A. Fox, M. Chanon (Eds.), Photoinduced Electron Transfer, Elsevier, Amsterdam, 1988, Part C.
[86] J.B. Lambert, W.J. Schulz Jr., in: S. Patai, Z. Rappoport (Eds.), The Chemistry of Organic Silicon Compounds, Wiley, Chichester, UK, 1989, chapter 16, p. 1007.
[87] C. Maerker, J. Kapp, P. von R. Schleyer, in: N. Auner, J. Weis (Eds.), Organosilicon Chemistry: From Molecules to Materials, vol. II, VCH, Weiheim, 1996, p. 326.
[88] J. Belzner, Angew. Chem., Int. Ed. Engl. 36 (1997) 1277.
[89] H. Schwarz, in: S. Patai, Z. Rappoport (Eds.), The Chemistry of Organic Silicon Compounds, Wiley, Chichester, UK, 1989, chapter 7, p. 445.
[90] P. von R. Schleyer, P. Buzek, T. Müller, Y. Apeloig, H.-U. Siehl, Angew. Chem., Int. Ed. Engl. 32 (1993) 1471.
[91] H.-U. Steinberger, T. Müller, N. Auner, C. Maerker, P. von R. Schleyer, Angew. Chem., Int. Ed. Engl. 36 (1997) 626.
[92] J.B. Lambert, Y. Zhao, Angew. Chem., Int. Ed. Engl. 36 (1997) 400.
[93] H. Bock, W. Kaim, M. Kira, R. West, J. Am. Chem. Soc. 26 (1979) 7667.
[94] T. Kudo, S. Nagase, Chem. Phys. Lett. 122 (1988) 233.
[95] C.J. Rhodes, J. Organomet. Chem. 443 (1993) 19.
[96] C. Glidewell, J. Organomet. Chem. 461 (1993) 15.
[97] C. Glidewell, C.J. Rhodes, J. Organomet. Chem. 471 (1994) 43.
[98] H. Preut, B. Mayer, W.P. Neumann, Acta Crystallogr. 39C (1983) 1118.
[99] H. Appler, L.W. Gross, B. Mayer, W.P. Neumann, J. Organomet. Chem. 291 (1985) 9.
[100] A. Sekiguchi, S. Ziegler, K.J. Haller, R. West, Rec. Trav. Chim. Pays-Bas 107 (1988) 197.
[101] W.S. Sheldrick, in: S. Patai, Z. Rappoport (Eds.), The Chemistry of Organic Silicon Compounds, Wiley, Chichester, UK, 1989, chapter 3, p. 227.
[102] H. Bock, B. Solouki, in: S. Patai, Z. Rappoport (Eds.), The Chemistry of Organic Silicon Compounds, Wiley, Chichester, UK, 1989, chaper 9, p. 555.
[103] D.N. Roak, G.J.D. Peddle, J. Am. Chem. Soc. 94 (1972) 5837.
[104] Y. Nakadaira, T. Otsuka, H. Sakurai, Tetrahedron Lett. 22 (1981) 2417.
[105] R.D. Rich, T.J. Drahnak, R. West, J. Michl, J. Organomet. Chem. 212 (1981) C1.
[106] M. Kako, M. Ninomiya, Y. Nakadaira, J. Chem. Soc., Chem. Commun. (1997) 1373.